



Common and dissociable effects of oxytocin and lorazepam on the neurocircuitry of fear

Ann-Kathrin Kreuder^a, Dirk Scheele^{a,b}, Johannes Schultz^c, Juergen Hennig^d, Nina Marsh^b, Torge Dellert^e, Ulrich Ettinger^f, Alexandra Philippsen^g, Mari Babasiz^a, Angela Herscheid^a, Laura Remmersmann^a, Ruediger Stirnberg^h, Tony Stöcker^{h,i}, and René Hurlmann^{a,b,j,1}

^aDivision of Medical Psychology, Department of Psychiatry and Psychotherapy, University Hospital Bonn, 53105 Bonn, Germany; ^bDepartment of Psychiatry, School of Medicine & Health Sciences, University of Oldenburg, 26129 Oldenburg, Germany; ^cCenter for Economics and Neuroscience, University of Bonn, 53113 Bonn, Germany; ^dDivision of Personality Psychology and Individual Differences, University of Giessen, 35390 Giessen, Germany; ^eInstitute of Medical Psychology and Systems Neuroscience, University of Muenster, 48149 Muenster, Germany; ^fDepartment of Psychology, University of Bonn, 53113 Bonn, Germany; ^gDepartment of Psychiatry and Psychotherapy, University Hospital Bonn, 53105 Bonn, Germany; ^hDivision of MR Physics, German Center for Neurodegenerative Diseases, 53175 Bonn, Germany; ⁱDepartment of Physics and Astronomy, University of Bonn, 53113 Bonn, Germany; and ^jResearch Center Neurosensory Science, University of Oldenburg, 26129 Oldenburg, Germany

Edited by Bruce S. McEwen, Rockefeller University, New York, NY, and approved March 31, 2020 (received for review November 15, 2019)

Benzodiazepines (BZDs) represent the gold standard of anxiolytic pharmacotherapy; however, their clinical benefit is limited by side effects and addictive potential. Consequently, there is an urgent need to develop novel and safe anxiolytics. The peptide hormone oxytocin (OXT) exhibits anxiolytic-like properties in animals and humans, but whether OXT and BZDs share similar effects on the neural circuitry of fear is unclear. Therefore, the rationale of this ultra-high-field functional MRI (fMRI) study was to test OXT against the clinical comparator lorazepam (LZP) with regard to their neuromodulatory effects on local and network responses to fear-related stimuli. One hundred twenty-eight healthy male participants volunteered in this randomized double-blind, placebo-controlled, between-group study. Before scanning using an emotional face-matching paradigm, participants were randomly administered a single dose of OXT (24 IU), LZP (1 mg), or placebo. On the behavioral level, LZP, but not OXT, caused mild sedation, as evidenced by a 19% increase in reaction times. On the neural level, both OXT and LZP inhibited responses to fearful faces vs. neutral faces within the centromedial amygdala (cmA). In contrast, they had different effects on intra-amygdalar connectivity; OXT strengthened the coupling between the cmA and basolateral amygdala, whereas LZP increased the interplay between the cmA and superficial amygdala. Furthermore, OXT, but not LZP, enhanced the coupling between the cmA and the precuneus and dorsomedial prefrontal cortex. These data implicate inhibition of the cmA as a common denominator of anxiolytic action, with only OXT inducing large-scale connectivity changes of potential therapeutic relevance.

amygdala | oxytocin | benzodiazepines | fear | fMRI

With a lifetime prevalence of >28% in the United States, anxiety disorders are the most frequent class of psychiatric diseases (1), imposing tremendous personal suffering and enormous socioeconomic costs (2). Even today, anxiety disorders are frequently treated with benzodiazepines (BZDs), which act as positive allosteric modulators through binding to gamma-aminobutyric acid A (GABA_A) receptors, thereby augmenting the inhibitory action of GABA (3). Amygdala hyperreactivity to threat signals has been discussed as a key neural substrate mediating the pathophysiology of inadequate fear responses in anxiety disorders (4, 5). Consistent with this model, previous neuroimaging studies have revealed that single-dose administration of BZDs diminishes amygdala responses to facial emotion in healthy subjects (6, 7). Beyond its clinically approved anxiolytic potential in humans (8), the use of BZDs is often hampered by acute adverse effects, including impaired cognitive and motor abilities, drowsiness, and dizziness, as well as dependence and withdrawal symptoms after long-term use (3). Considering the adverse effects of BZDs and the considerable number of patients with treatment-resistant anxiety (9), new

compounds that target and modulate the neurocircuitry of fear are needed.

Currently, several peptide neuromodulators are being trialed for their anxiolytic efficacy, including the hypothalamic peptide oxytocin (OXT), which has anxiolytic-like properties by inhibiting amygdala responses to fear signals in patients with anxiety disorders (10) and healthy subjects (11–14). By demonstrating OXT-induced target engagement, as evidenced by a dose-dependent reduction in fear-related amygdala activity in male subjects (15), an initial step in translating OXT to the clinic, as recommended by the National Institute of Mental Health roadmap (16), has been achieved. The present study aimed to initiate the next step toward the clinical translation of OXT as a novel anxiolytic agent by testing the neuromodulatory effects of OXT against those of a clinical comparator, the high-potency 3-hydroxy BZD lorazepam (LZP), on amygdala reactivity and functional connectivity in humans.

To develop effective anxiolytics, the neurocircuitry regulating fear must be considered, and current concepts emphasize a key role of the functional organization within the amygdala complex (17). A plethora of animal studies have revealed that the basolateral amygdala (bLA), composed of the lateral, basal, and accessory basal nuclei (18), and the centromedial amygdala (cmA),

Significance

A potential new target for anxiolytic drug development is the oxytocin (OXT) neuropeptide system. An emerging question is whether OXT has similar effects on the neural microcircuitry of fear compared with clinically established compounds such as benzodiazepines. The present functional MRI study showed that both OXT and its benzodiazepine comparator lorazepam (LZP) reduced centromedial amygdala responses to fear signals. OXT, but not LZP, increased extra-amygdalar connectivity between the centromedial amygdala and frontoparietal regions. Thus, while both compounds inhibited the centromedial amygdala, OXT, but not LZP, elicited large-scale connectivity changes of potential therapeutic relevance.

Author contributions: A.-K.K., D.S., J.S., and R.H. designed research; A.-K.K., N.M., T.D., M.B., A.H., L.R., and R.H. performed research; R.S. and T.S. contributed new reagents/analytic tools; A.-K.K., D.S., J.S., and R.H. analyzed data; and A.-K.K., D.S., J.S., J.H., N.M., T.D., U.E., A.P., M.B., A.H., L.R., R.S., T.S., and R.H. wrote the paper.

The authors declare no competing interest.

This article is a PNAS Direct Submission.

Published under the PNAS license.

¹To whom correspondence may be addressed. Email: renehurlmann@icloud.com.

This article contains supporting information online at <https://www.pnas.org/lookup/suppl/doi:10.1073/pnas.1920147117/-DCSupplemental>.

First published May 8, 2020.

composed of the medial and central nuclei (18), play pivotal roles in the formation and regulation of fear (4). Information from the unimodal and polymodal sensory cortices, thalamus, hippocampus, and prefrontal cortex (PFC) enters the amygdala via the blA and is subsequently conveyed to the cmA (17). Neurons in the blA encode the threat value of an incoming stimulus (17), and the cmA mediates species-specific behavioral and physiological responses to such stimuli through projections to the brainstem, hypothalamus, and basal forebrain (4). In addition, the cortical nuclei of the amygdala and the nucleus of the olfactory tract compose the superficial amygdala (sfA) (18). The sfA has been linked to intraspecies communication in vertebrates (19) and to social information processing and approach-avoidance behavior in humans (20).

While the intra- and extra-amygdalar pathways regulating fear have been accurately mapped in animals using optogenetics (21, 22), the anxiolytic mechanisms within the human amygdala subarchitecture, which could be targeted by new compounds and could enable individually tailored treatment protocols, have received less attention. Furthermore, studies in animals have identified amygdalar subnuclei-specific anxiolytic mechanisms of OXT (23) and LZP (24), but the anxiolytic mechanisms of both compounds within the human amygdala subarchitecture have not been examined due to critical methodological requirements.

Therefore, using ultra-high-field imaging, we conducted this randomized, placebo-controlled (PLC), double-blind, between-group functional magnetic resonance imaging (fMRI) study involving 128 healthy males aimed to precisely map and compare the OXT (24 IU) and LZP (1 mg) effects on amygdalar sub-region responses to fear-related stimuli (Fig. 1). In addition, we sought to characterize the effects of OXT and LZP on intra- and extra-amygdalar functional connectivity while processing fear-related stimuli to discern local and network effects. During the scan, an emotional face-matching task (25) was performed

(Fig. 2A) that produces robust amygdala activity (26–28), is sensitive to the effects of OXT (10, 11) and LZP (6) on amygdala activity, and elicits increased amygdala activation in patients with anxiety disorders (10, 29).

Results

Behavioral Results. A mixed analysis of variance with the within-subjects factor “stimulus category” (fearful, happy, neutral, house), the between-subjects factor “treatment” (OXT, LZP, PLC) and reaction times (in seconds) as the dependent variable was performed. This ANOVA yielded main effects of stimulus category ($F_{(3, 345)} = 9.68, P < 0.001, \eta_p^2 = 0.08$) and treatment ($F_{(2,115)} = 6.54, P = 0.002, \eta_p^2 = 0.10$). Post hoc paired *t* tests showed that participants reacted significantly faster to fearful faces (1.31 ± 0.35) compared with happy faces ($1.41 \pm 0.40; t_{(117)} = -5.13, P_{corr} < 0.001, d = -0.26$), neutral faces ($1.44 \pm 0.40; t_{(117)} = -6.54, P_{corr} < 0.001, d = -0.32$), and houses ($1.38 \pm 0.37; t_{(117)} = -2.71, P_{corr} = 0.048, d = -0.18$). In addition, the administration of LZP (1.57 ± 0.41) resulted in increased reaction times to all stimuli compared with OXT ($1.30 \pm 0.25; t_{(57)} = -2.91, P_{corr} = 0.015, d = -0.76$) and PLC ($1.32 \pm 0.32; t_{(89)} = -3.13, P_{corr} = 0.006, d = -0.69$) (Fig. 2B). Moreover, there was no significant interaction between stimulus category and treatment ($F_{(6, 345)} = 0.63, P = 0.71, \eta_p^2 = 0.01$), and no treatment effect on the percentage of correct responses ($P \geq 0.05$ for all) (SI Appendix, Results).

fMRI Results. We analyzed the neural response to fearful faces vs. neutral faces as a task effect in the PLC group and found whole-brain activations in the right posterior cingulate cortex (Montreal Neurological Institute [MNI] peak coordinates: *x, y, z*: 3, -47, 27; $k_e = 93, t_{(224)} = 4.34, P_{FWE} < 0.001$) and right middle temporal gyrus (52, -41, 8; $k_e = 52, t_{(224)} = 4.17, P_{FWE} = 0.049$) (SI Appendix, Table S2). Furthermore, a region of interest (ROI)-based

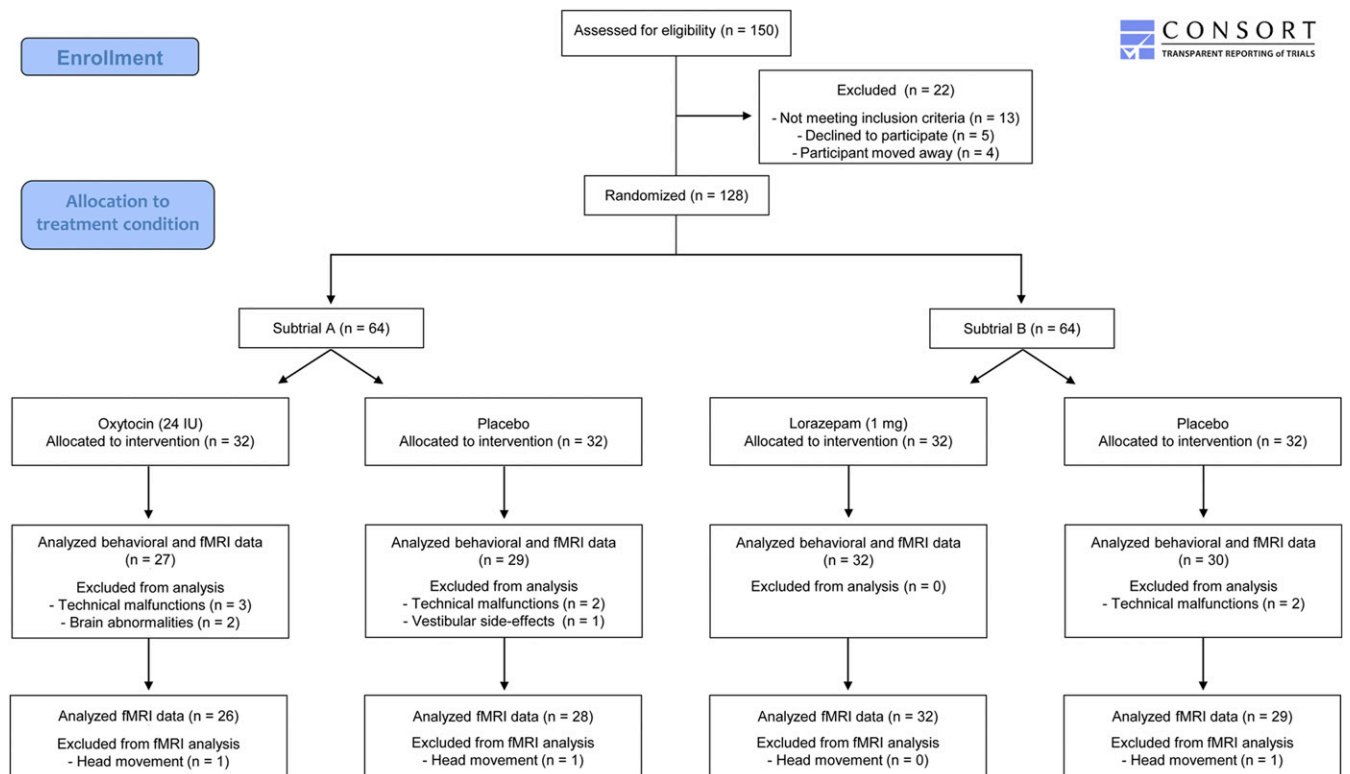


Fig. 1. Flow of participants through the trial.

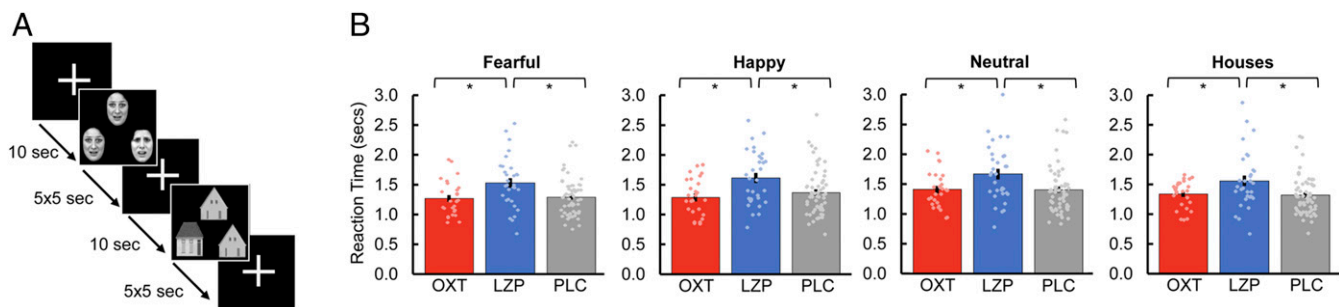


Fig. 2. During ultra-high-field fMRI (7-T), subjects were exposed to an adapted version of a well-established emotional face-matching task. (A) Participants viewed either a trio of emotional faces (fearful, happy, neutral) or houses as nonsocial control stimuli, and were instructed to select the face (or house) in the bottom row that was identical to the target stimulus. (B) The administration of LZP resulted in a significant increase in reaction time in all stimulus categories compared with transnasal OXT ($t_{(57)} = -2.91$, $P_{corr} = 0.015$, $d = -0.76$) and PLC ($t_{(89)} = -3.13$, $P_{corr} = 0.006$, $d = -0.69$). Furthermore, the reaction time to fearful faces was significantly shorter compared with happy faces ($t_{(117)} = -5.13$, $P_{corr} < 0.001$, $d = -0.26$), neutral faces ($t_{(117)} = -6.54$, $P_{corr} < 0.001$, $d = -0.32$), and houses ($t_{(117)} = -2.71$, $P_{corr} = 0.048$, $d = -0.18$) across treatment groups. Error bars indicate SEM. * $P_{corr} < 0.05$.

analysis revealed that fearful faces significantly increase activity in the left cmA relative to neutral faces ($-22, -12, -14$; $t_{(224)} = 4.41$, $P_{FWE} = 0.001$).

Importantly, compared with PLC, both intranasal OXT ($-22, -12, -14$; $t_{(224)} = 3.69$, $P_{FWE} = 0.008$) and LZP ($-24, -7, -14$; $t_{(224)} = 3.85$, $P_{FWE} = 0.005$) significantly reduced the neural response to fearful faces vs. neutral faces in the left cmA (Fig. 3). A direct comparison between the effects of OXT and LZP on intra-amygdalar activity during the processing of fearful faces revealed a more pronounced reduction of neural activity in a posterior subpart of the cmA under the influence of OXT ($-22, -12, -14$; $t_{(224)} = 3.10$, $P_{FWE} = 0.047$).

Functional Connectivity. The generalized psychophysiological interactions analyses revealed treatment-specific modulations of intra-amygdalar connectivity in response to fearful faces relative to neutral faces. OXT significantly increased the connectivity between the right cmA (seed region) and the left blA ($-19, -3, -19$; $t_{(224)} = 3.92$, $P_{FWE} = 0.009$) (Fig. 4A) compared with PLC, whereas LZP significantly strengthened the connectivity between the left cmA (seed region) and the right sFA ($15, -8, -16$; $t_{(224)} = 3.29$, $P_{FWE} = 0.029$) (Fig. 4B) compared with PLC. In addition, the analysis showed a selective effect of OXT on extra-amygdalar functional coupling in response to fearful faces vs. neutral faces. Intranasal OXT relative to PLC augmented the connectivity between the right cmA (seed region) and the left precuneus ($-7, -44, 66$; $k_c = 63$, $t_{(224)} = 4.18$, $P_{FWE} = 0.003$) (Fig. 5A) and between the left cmA (seed region) and the

left dorsomedial PFC (dmPFC; $-12, 48, 24$; $k_c = 41$, $t_{(224)} = 4.55$, $P_{FWE} = 0.036$) (Fig. 5B). Treatment effects on amygdalar sub-region responses and intra- and extra-amygdalar connectivity to happy faces vs. neutral faces and to faces vs. houses are reported in *SI Appendix*.

Discussion

This study sought to decipher and compare the effects of OXT and LZP on fear-related activity and connectivity in distinct subregions of the human amygdala using functional ultra-high-field MRI. Crucially, the study provides the first evidence that the two compounds share comparable effects on amygdala subarchitecture activity in response to fear-related stimuli but elicit distinct effects on small- and large-scale neural networks.

Specifically, we found that both OXT and LZP reduce responses to fearful faces relative to neutral faces within the cmA, indicating an evolutionarily conserved anxiolytic mechanism across rodents and humans. Animal studies have identified the central amygdalar nucleus (CeA), which is part of the cmA subregion, as the primary site for BZD-dependent anxiolytic action via activation of GABAergic neurons (24, 30), resulting in inhibited transmission of aversive signals through the CeA (31). Likewise, OXT decreases anxiety-related behavior by activating GABAergic inhibitory neurons originating from the lateral CeA, which reduces the excitability of neurons in the medial CeA (32, 33). Interestingly, in rats, the infusion of OXT enhances the inhibitory effects of BZDs in the medial CeA, implicating that the anxiolytic effects of OXT and BZDs could be attributed to the

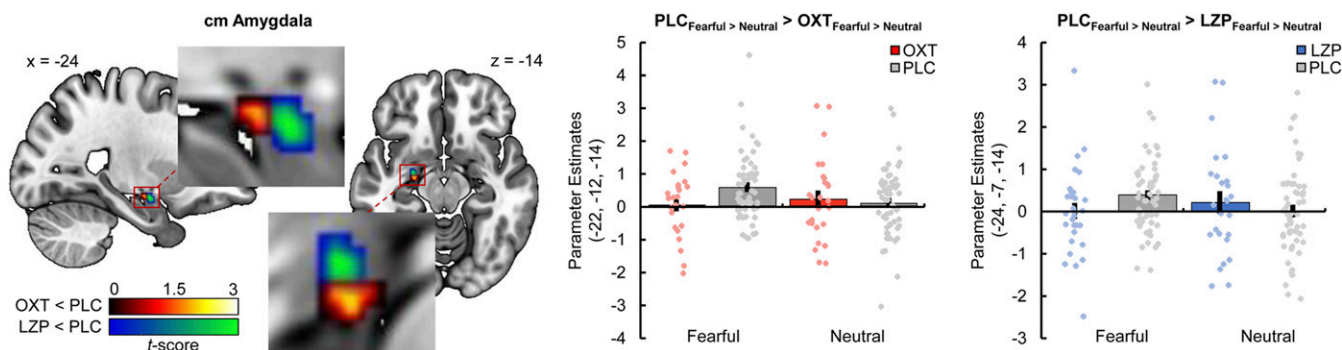


Fig. 3. Both intranasal OXT (peak MNI coordinates x, y, z : $-22, -12, -14$; $t_{(224)} = 3.69$, $P_{FWE} = 0.008$, display threshold $P < 0.05$ uncorrected) and LZP ($-24, -7, -14$; $t_{(224)} = 3.85$, $P_{FWE} = 0.005$, display threshold $P < 0.05$ uncorrected) significantly diminished the neural response to fearful relative to neutral faces in the left cmA compared with PLC (OXT < PLC, red-yellow cluster; LZP < PLC, blue-green cluster). Error bars indicate the SEM.

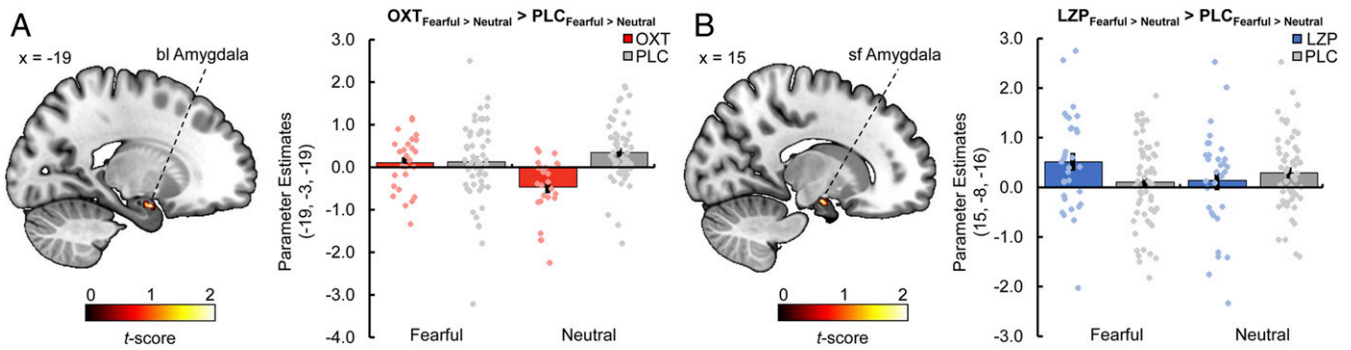


Fig. 4. (A) Compared with PLC, intranasal OXT increased the intra-amygdala functional connectivity between the right cmA as a seed region and the left blA during the processing of fearful relative to neutral faces (peak MNI coordinates x, y, z : $-19, -3, -19$; $t_{(224)} = 3.92$, $P_{FWE} = 0.009$, display threshold $P < 0.05$ uncorrected). (B) Compared with PLC, the administration of LZP resulted in enhanced intra-amygdala functional connectivity between the left cmA (seed region) and the right sfA in response to fearful faces vs. neutral faces ($15, -8, -16$; $t_{(224)} = 3.29$, $P_{FWE} = 0.029$, display threshold $P < 0.05$ uncorrected). Error bars indicate SEM.

modulation of the same GABAergic circuit (24). Novel compounds that could enhance the GABAergic function are being discussed as a promising approach for the treatment of anxiety (3). Thus, future human studies are warranted to probe whether OXT could augment the anxiolytic effects of BZDs by elevating the GABAergic tone within the amygdala microcircuitry.

Furthermore, animal models have corroborated a considerable involvement of the intra- and extra-amygdalar connectivity in the regulation of fear (17). Our study revealed treatment-specific effects on intra-amygdalar connectivity. On the one hand, LZP increased functional connectivity between the cmA and the sfA in response to fearful faces relative to neutral faces. The sfA has been associated with the modulation of approach-avoidance behavior (20) and BZDs increase social approach behavior (34). Thus, LZP may modulate anxiety-related behavior by reducing avoidance behavior through a reduction of cmA activity and by concomitantly inducing social exploration through enhanced connectivity between the cmA and sfA.

On the other hand, OXT significantly elevated the functional connectivity between the cmA and the blA while processing fearful relative to neutral faces. Optogenetic stimulation of blA terminals in the CeA has strong anxiolytic effects (21), and blA activity in humans has been found to predict subsequent activity in the cmA (35), which corresponds to the intra-amygdalar connectivity pattern derived from animal models (17, 36). Thus, by strengthening the functional connectivity between the cmA and the blA, OXT may enhance the feed-forward inhibition of the cmA via the blA (21), leading to diminished fear

responses. Considering the treatment-specific effects on intra-amygdalar connectivity, we hypothesize that dual administration of OXT and LZP might target two core symptoms of anxiety disorders: clinically elevated avoidance behavior (37) and fear response (4).

Importantly, OXT selectively strengthened fear-related functional interplay between the cmA and the dmPFC. The blA is highly interconnected with the PFC (17), and OXT-induced increased functional connectivity between the amygdala and PFC may reflect an enhanced top-down cognitive control that has previously been observed in the context of social pain modulation (38). Moreover, patients with anxiety disorders exhibit decreased functional connectivity between the CeA and PFC (39), supporting the idea of amygdala hyperactivity (5) and PFC hypoactivity (40) as a neural endophenotype of anxiety disorders. Our results indicate that OXT could reduce anxiety-related behavior by decreasing cmA activity and concomitantly modulating polysynaptic PFC-amygdalar subregion pathways.

In addition, we detected an OXT-dependent increase in functional coupling between the cmA and the precuneus while processing fearful faces relative to neutral faces. This observation is in line with previous findings that OXT increases the functional connectivity between the amygdala and the precuneus during the processing of social stimuli (41). In contrast, OXT seems to decrease resting-state functional connectivity between the cmA and the precuneus in the absence of external social stimuli (42), supporting the idea of context-specific modulatory effects of OXT (43, 44). Besides its role in self-consciousness and

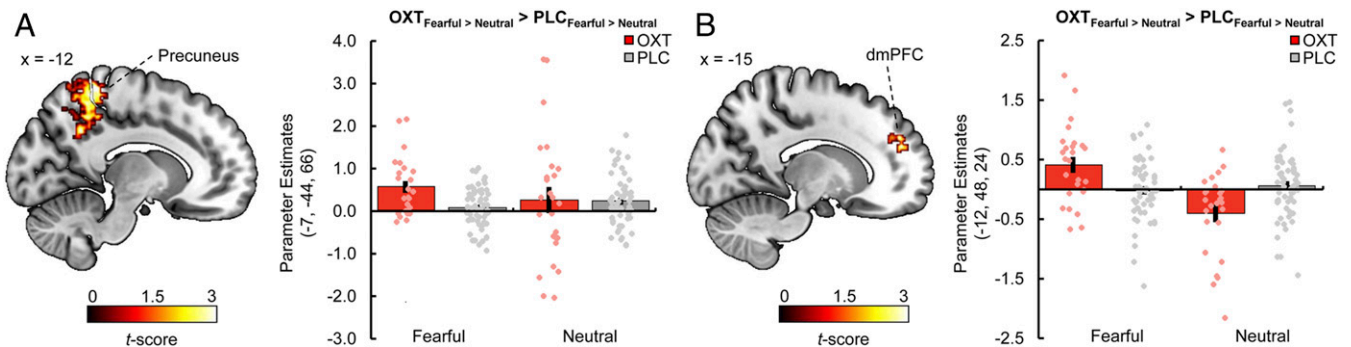


Fig. 5. (A) Compared with PLC, intranasal OXT significantly enhanced the functional connectivity between the right cmA as a seed region and the left precuneus during the processing of fearful faces vs. neutral faces (peak MNI coordinates x, y, z : $-7, -44, 66$; $k_e = 63$, $t_{(224)} = 4.18$, $P_{FWE} = 0.003$, display threshold $P < 0.001$ uncorrected). (B) OXT also increased the functional connectivity between the left cmA (seed region) and the left dmPFC during the processing of fearful faces vs. neutral faces ($-12, 48, 24$; $k_e = 41$, $t_{(224)} = 4.55$, $P_{FWE} = 0.036$, display threshold $P < 0.001$ uncorrected). Error bars indicate SEM.

self-referential processing (45), the precuneus has been implicated in the processing of social stimuli (46). Consequently, by strengthening the functional coupling between the cmA and the precuneus, OXT may enhance the salience of social stimuli (47).

A higher dose of BZDs could produce a more potent anxiolytic effect, while 24 IU of OXT has been identified as the most effective OXT dose to reduce amygdala activation (15). However, given the distinct anxiolytic mechanisms of both treatments and the specific OXT effects on large-scale neural networks, we hypothesize that the oxytocinergic augmentation of BZD-based antianxiety treatments could open new avenues for an improved dosage titration of BZDs. Eventually, OXT as an adjunct may help reduce adverse effects and lower the risk of dependence in the treatment of anxiety disorders.

On the behavioral level, we observed that LZP significantly increased the reaction times to all emotional stimuli, most likely related to mild sedation mediated by the binding of classical BZDs to the α_1 -subunit of the GABA_A receptor (2, 3). Consistent with previous imaging studies investigating the effects of OXT on emotional face processing (10–13, 15), our study did not reveal any modulatory effects of intranasal OXT on reaction times during the fMRI task or any change in accuracy ratings (*SI Appendix, Results*). While ceiling effects in the behavioral data may have hindered the detection of OXT-ergic modulation in the present study, behavioral OXT effects have previously been reported in reaction to more complex social stimuli related to pair-bonding or attachment (38, 48–51). Importantly, the emotional face-matching task in our study was primarily designed not to produce sensitive behavioral markers for emotional face processing, but rather to evoke robust and reliable amygdala activation.

The present study has several limitations. First, the sample was limited to male participants. Considering the evidence for a more prevalent use of anxiolytics in females (52, 53) and for sex-specific effects of OXT on amygdala activity (54), which might be based on interactions with sexual steroids (55, 56), future research is needed to examine the effects of OXT and LZP on amygdalar subarchitecture responses in females. Second, our study sample consisted of healthy volunteers without current or past psychiatric illness; future studies should investigate the effects of OXT and LZP on fear-related amygdala subregion activity in patients with anxiety disorders. Third, although emotional face-processing tasks have illustrated dysfunctional neurobiological mechanisms in anxiety disorders (57), the common and distinct effects of OXT and LZP on clinical and psychophysiological assessments of threat reactivity must be determined. Fourth, while the detection of fear signals is a key function of the amygdala (58), accumulating evidence indicates that the amygdala is part of a large-scale salience network that also includes the anterior insula and anterior cingulate cortex (59). Consequently, future studies are needed to disentangle fear- and salience-related effects of LZP and OXT.

Our data provide insight into the intra-amygdalar mechanisms of OXT and its clinical comparator LZP in humans, thereby facilitating the development of individually adjusted treatment strategies based on the distinct anxiolytic mechanisms of both compounds. Collectively, OXT and LZP dampened the responses to fear-related stimuli in the cmA as a central hub of anxiolytic action, with only OXT inducing large-scale connectivity changes of potential therapeutic relevance.

Materials and Methods

Participants and Experimental Design. A total of 128 nonsmoking, right-handed, healthy males (mean age, 25.67 ± 4.32 y) volunteered for this study and provided written informed consent. The present study focused on male subjects to control for interaction effects between OXT and sex steroids (55). Subjects were recruited using online advertisements and public postings and were free of past and current physical or psychiatric illness, as

assessed by medical history and the Mini-International Neuropsychiatric Interview (60) in a screening session before the fMRI session. Subjects reported low levels of depressive symptoms, as well as low levels of anxiety and autistic traits (*SI Appendix, Table S1*).

The present fMRI study consisted of two subtrials, A and B, each a priori designed for between-group comparisons. This particular design accounted for potential subjective side effects associated with LZP, including dizziness and sedation, which usually do not occur to such a degree in OXT studies (61) and were due to different dose–response kinetics across compounds. In subtrial A, participants were randomly assigned to receive either intranasal OXT (24 IU; six puffs of 2 IU per nostril; Novartis) or PLC. In subtrial B, participants were randomly assigned to receive either oral LZP (1 mg; Pfizer Pharma) or PLC. The PLC contained all ingredients except the active agent. Importantly, for the selected doses of intranasal OXT (24 IU) (15) and oral LZP (1 mg) (6), previous studies have reported reduced amygdala activity in response to emotional faces. In addition, a daily LZP dose of 1 to 4 mg orally is clinically established for the treatment of anxiety (62). For the purpose of reducing unintended side effects, we chose a dose at the lower end of the clinically used LZP doses to treat anxiety.

After drug administration, 10 subjects dropped out due to technical malfunctions ($n = 7$), anatomic brain abnormalities ($n = 2$), or vestibular side effects ($n = 1$). Since the statistical analysis of the behavioral and the neural data (whole-brain and ROI-based approaches) did not reveal significant differences between the two PLC groups ($P \geq 0.05$ for all), we aggregated them for the subsequent analyses. Thus, the final sample included 27 subjects treated with OXT, 32 subjects treated with LZP, and 59 subjects receiving PLC. Three subjects had to be excluded from fMRI data analyses due to excessive head movements during scanning (Fig. 1). To accommodate the different dose–response kinetics, fMRI scanning commenced 30 min after treatment in subtrial A and 90 min after treatment in subtrial B (*SI Appendix, Methods*).

There were no a priori differences in demographic and psychometric variables between the treatment groups (*SI Appendix, Table S1*).

The study was approved by the Institutional Review Board of the Medical Faculty of the University Hospital Bonn and was conducted in accordance with the Declaration of Helsinki. Further information on study procedures, fMRI acquisition, and data analysis is provided in *SI Appendix*.

fMRI Paradigm. We applied an adapted version of a well-established emotional face-matching paradigm (25) to examine the effects of OXT and LZP on amygdalar subregion activity in response to emotional faces. During fMRI scanning, a trio of either black and white scaled emotional faces or houses (= nonsocial control stimuli) were presented on a 32-inch MRI-compatible TFT/LCD monitor (Medres, Cologne, Germany) using Presentation version 14 (Neurobehavioral Systems). The participants were instructed to choose the face or house in the bottom row that was identical with the target stimulus in the top row by pressing one of two buttons on an MRI-compatible response pad. The paradigm consisted of 12 blocks (three blocks of each stimulus category: houses, fearful, happy, and neutral faces) with five trios per block displayed for 5 s each (Fig. 2A). The block order was randomized, with blocks interleaved with a 10-s interstimulus interval showing a white fixation cross depicted at the screen center. Face stimuli were obtained from the Karolinska Directed Emotional Faces database (63).

Image Acquisition. A 7-T whole-body MRI research system (Siemens Healthineers) with a 32-channel head array coil (32Rx/1Tx; Nova Medical) was used to obtain T2*-weighted whole-brain images with blood oxygen level-dependent contrast at 1.7-mm isotropic resolution using an accelerated 3D echo planar imaging sequence (64, 65) (*SI Appendix, Methods*).

Statistical Analysis. MRI data were processed and analyzed using SPM12 software (Wellcome Trust Center for Neuroimaging; <http://www.fil.ion.ucl.ac.uk/spm>) implemented in MATLAB (MathWorks) (*SI Appendix, Methods*). A two-level random-effects approach based on the general linear model was used for statistical analyses. On the first level, four conditions (fearful, happy, neutral, house) were modeled by a boxcar function convolved with a hemodynamic response function (66). Button presses were modeled as regressors of no interest. Movement parameters and nuisance regressors for physiological noise correction were entered as confounders in the design matrix (*SI Appendix, Methods*). On the second level, a full-factorial design with the between-subjects factor “treatment” and the within-subjects factor “emotion category” was conducted.

Based on the study rationale, the bIA, cmA, and sfA were defined as ROIs based on cytoarchitectonic probabilistic maps (67) implemented in the Anatomy toolbox (68). The significance threshold for these ROI analyses was

set to $P < 0.05$, familywise error-corrected for multiple comparisons based on the size of the ROI. In addition, an exploratory whole-brain analysis was performed (cluster defining threshold $P < 0.001$; significance threshold $P_{FWE} < 0.05$ corrected).

To further address the effects of treatment on functional connectivity (i.e., temporal synchrony of blood oxygenation level-dependent activation in a seed region and a target area), we conducted generalized psychophysiological interactions analyses (69). Based on the results of the ROI analysis, we examined the effects of OXT and LZP on the extra- and intra-amygdalar functional connectivity of the cmA. The bilateral cmA were defined as seed regions using the cytoarchitectonic probabilistic maps of the Anatomy toolbox (67, 68). To determine the direction and specificity of the OXT and LZP effects, the MarsBaR toolbox (<http://marsbar.sourceforge.net/>) was used

to extract parameter estimates from the voxel cluster showing significant effects.

Behavioral data were analyzed using SPSS version 24 (IBM). Quantitative behavioral data were compared using mixed ANOVA and follow-up t tests. All reported P values are two-tailed and Bonferroni-corrected (P_{corr}). Partial η^2 and Cohen's d were calculated as measures of effect size.

Data Availability. Data for this manuscript will be made available upon request.

ACKNOWLEDGMENTS. We thank Paul Jung for excellent programming assistance and Alexandra Patin for proofreading the manuscript.

1. R. C. Kessler et al., Lifetime prevalence and age-of-onset distributions of DSM-IV disorders in the National Comorbidity Survey Replication. *Arch. Gen. Psychiatry* **62**, 593–602 (2005). Correction in: *Arch. Gen. Psychiatry* **62**, 768 (2005).
2. N. S. Pillay, D. J. Stein, Emerging anxiolytics. *Expert Opin. Emerg. Drugs* **12**, 541–554 (2007).
3. D. H. Farb, M. H. Ratner, Targeting the modulation of neural circuitry for the treatment of anxiety disorders. *Pharmacol. Rev.* **66**, 1002–1032 (2014).
4. A. Etkin, Functional neuroanatomy of anxiety: A neural circuit perspective. *Curr. Top. Behav. Neurosci.* **2**, 251–277 (2010).
5. A. Etkin, T. D. Wager, Functional neuroimaging of anxiety: A meta-analysis of emotional processing in PTSD, social anxiety disorder, and specific phobia. *Am. J. Psychiatry* **164**, 1476–1488 (2007).
6. M. P. Paulus, J. S. Feinstein, G. Castillo, A. N. Simmons, M. B. Stein, Dose-dependent decrease of activation in bilateral amygdala and insula by lorazepam during emotion processing. *Arch. Gen. Psychiatry* **62**, 282–288 (2005).
7. C. M. Del-Ben et al., Effects of diazepam on BOLD activation during the processing of aversive faces. *J. Psychopharmacol.* **26**, 443–451 (2012).
8. E. J. Hoffman, S. J. Mathew, Anxiety disorders: A comprehensive review of pharmacotherapies. *Mt. Sinai J. Med.* **75**, 248–262 (2008).
9. A. Bystritsky, Treatment-resistant anxiety disorders. *Mol. Psychiatry* **11**, 805–814 (2006).
10. I. Labuschagne et al., Oxytocin attenuates amygdala reactivity to fear in generalized social anxiety disorder. *Neuropsychopharmacology* **35**, 2403–2413 (2010).
11. P. Kirsch et al., Oxytocin modulates neural circuitry for social cognition and fear in humans. *J. Neurosci.* **25**, 11489–11493 (2005).
12. M. Gamer, B. Zuroski, C. Büchel, Different amygdala subregions mediate valence-related and attentional effects of oxytocin in humans. *Proc. Natl. Acad. Sci. U.S.A.* **107**, 9400–9405 (2010).
13. G. Domes et al., Oxytocin attenuates amygdala responses to emotional faces regardless of valence. *Biol. Psychiatry* **62**, 1187–1190 (2007).
14. S. Radke et al., Oxytocin reduces amygdala responses during threat approach. *Psychoneuroendocrinology* **79**, 160–166 (2017).
15. F. B. Spengler et al., Kinetics and dose dependency of intranasal oxytocin effects on amygdala reactivity. *Biol. Psychiatry* **82**, 885–894 (2017).
16. T. R. Insel, Translating oxytocin neuroscience to the clinic: A National Institute of Mental Health Perspective. *Biol. Psychiatry* **79**, 153–154 (2016).
17. G. G. Calhoun, K. M. Tye, Resolving the neural circuits of anxiety. *Nat. Neurosci.* **18**, 1394–1404 (2015).
18. P. Sah, E. S. Faber, M. Lopez De Armentia, J. Power, The amygdaloid complex: Anatomy and physiology. *Physiol. Rev.* **83**, 803–834 (2003).
19. N. Moreno, A. González, Evolution of the amygdaloid complex in vertebrates, with special reference to the anamnio-amniotic transition. *J. Anat.* **211**, 151–163 (2007).
20. D. Bzdok, A. R. Laird, K. Zilles, P. T. Fox, S. B. Eickhoff, An investigation of the structural, connective, and functional subspecialization in the human amygdala. *Hum. Brain Mapp.* **34**, 3247–3266 (2013).
21. K. M. Tye et al., Amygdala circuitry mediating reversible and bidirectional control of anxiety. *Nature* **471**, 358–362 (2011).
22. S. Ciochi et al., Encoding of conditioned fear in central amygdala inhibitory circuits. *Nature* **468**, 277–282 (2010).
23. D. Viviani et al., Oxytocin selectively gates fear responses through distinct outputs from the central amygdala. *Science* **333**, 104–107 (2011).
24. D. Viviani, T. Terrettaz, F. Magara, R. Stoop, Oxytocin enhances the inhibitory effects of diazepam in the rat central medial amygdala. *Neuropharmacology* **58**, 62–68 (2010).
25. A. R. Hariri et al., Serotonin transporter genetic variation and the response of the human amygdala. *Science* **297**, 400–403 (2002).
26. E. M. Drabant, K. McRae, S. B. Manuck, A. R. Hariri, J. J. Gross, Individual differences in typical reappraisal use predict amygdala and prefrontal responses. *Biol. Psychiatry* **65**, 367–373 (2009).
27. P. M. Fisher et al., Medial prefrontal cortex 5-HT(2A) density is correlated with amygdala reactivity, response habituation, and functional coupling. *Cereb. Cortex* **19**, 2499–2507 (2009).
28. R. Sladky et al., High-resolution functional MRI of the human amygdala at 7 T. *Eur. J. Radiol.* **82**, 728–733 (2013).
29. K. E. Prater, A. Hosanagar, H. Klumpp, M. Angstadt, K. L. Phan, Aberrant amygdala-frontal cortex connectivity during perception of fearful faces and at rest in generalized social anxiety disorder. *Depress. Anxiety* **30**, 234–241 (2013).
30. M. C. Carvalho, C. M. Moreira, J. M. Zanoveli, M. L. Brandão, Central, but not basolateral, amygdala involvement in the anxiolytic-like effects of midazolam in rats in the elevated plus maze. *J. Psychopharmacol.* **26**, 543–554 (2012).
31. J. Griessner et al., Central amygdala circuit dynamics underlying the benzodiazepine anxiolytic effect. *Mol. Psychiatry*, 10.1038/s41380-018-0310-3 (2018).
32. D. Huber, P. Veinante, R. Stoop, Vasopressin and oxytocin excite distinct neuronal populations in the central amygdala. *Science* **308**, 245–248 (2005).
33. H. S. Knobloch et al., Evoked axonal oxytocin release in the central amygdala attenuates fear response. *Neuron* **73**, 553–566 (2012).
34. L. B. Nicolas, E. P. Prinszen, Social approach-avoidance behavior of a high-anxiety strain of rats: Effects of benzodiazepine receptor ligands. *Psychopharmacology* **184**, 65–74 (2006).
35. M. M. Grant et al., Influence of early life stress on intra- and extra-amygdaloid causal connectivity. *Neuropsychopharmacology* **40**, 1782–1793 (2015).
36. O. Babaev, C. Piletti Chatain, D. Krueger-Burg, Inhibition in the amygdala anxiety circuitry. *Exp. Mol. Med.* **50**, 18 (2018).
37. R. L. Aupperle, M. P. Paulus, Neural systems underlying approach and avoidance in anxiety disorders. *Dialogues Clin. Neurosci.* **12**, 517–531 (2010).
38. A. K. Kreuder et al., Oxytocin enhances the pain-relieving effects of social support in romantic couples. *Hum. Brain Mapp.* **40**, 242–251 (2019).
39. R. M. Birn et al., Evolutionarily conserved prefrontal-amygdalar dysfunction in early-life anxiety. *Mol. Psychiatry* **19**, 915–922 (2014).
40. S. Bishop, J. Duncan, M. Brett, A. D. Lawrence, Prefrontal cortical function and anxiety: Controlling attention to threat-related stimuli. *Nat. Neurosci.* **7**, 184–188 (2004).
41. M. Eckstein et al., Oxytocin facilitates the extinction of conditioned fear in humans. *Biol. Psychiatry* **78**, 194–202 (2015).
42. J. Kumar, B. Völlm, L. Palaniyappan, Oxytocin affects the connectivity of the precuneus and the amygdala: A randomized, double-blinded, placebo-controlled neuroimaging trial. *Int. J. Neuropsychopharmacol.* **18**, 1–7 (2014).
43. J. A. Bartz, J. Zaki, N. Bolger, K. N. Ochsner, Social effects of oxytocin in humans: Context and person matter. *Trends Cogn. Sci.* **15**, 301–309 (2011).
44. M. Olf et al., The role of oxytocin in social bonding, stress regulation and mental health: An update on the moderating effects of context and interindividual differences. *Psychoneuroendocrinology* **38**, 1883–1894 (2013).
45. M. Cabanis et al., The precuneus and the insula in self-attributional processes. *Cogn. Affect. Behav. Neurosci.* **13**, 330–345 (2013).
46. M. Amft et al., Definition and characterization of an extended social-affective default network. *Brain Struct. Funct.* **220**, 1031–1049 (2015).
47. S. G. Shamay-Tsoory, A. Abu-Akel, The social salience hypothesis of oxytocin. *Biol. Psychiatry* **79**, 194–202 (2016).
48. D. Scheele et al., Oxytocin enhances brain reward system responses in men viewing the face of their female partner. *Proc. Natl. Acad. Sci. U.S.A.* **110**, 20308–20313 (2013).
49. D. Scheele et al., An oxytocin-induced facilitation of neural and emotional responses to social touch correlates inversely with autism traits. *Neuropsychopharmacology* **39**, 2078–2085 (2014).
50. D. Scheele et al., Oxytocin modulates social distance between males and females. *J. Neurosci.* **32**, 16074–16079 (2012).
51. A. K. Kreuder et al., How the brain codes intimacy: The neurobiological substrates of romantic touch. *Hum. Brain Mapp.* **38**, 4525–4534 (2017).
52. J. Alonso et al.; ESEMeD/MHEDEA 2000 Investigators, European Study of the Epidemiology of Mental Disorders (ESEMeD) Project, Psychotropic drug utilization in Europe: Results from the European Study of the Epidemiology of Mental Disorders (ESEMeD) project. *Acta Psychiatr. Scand. Suppl.* **420** (suppl.), 55–64 (2004).
53. J. H. Van der Heyden et al., Gender differences in the use of anxiolytics and antidepressants: A population-based study. *Pharmacoepidemiol. Drug Saf.* **18**, 1101–1110 (2009).
54. G. Domes et al., Effects of intranasal oxytocin on emotional face processing in women. *Psychoneuroendocrinology* **35**, 83–93 (2010).
55. D. Scheele, J. Plota, B. Stoffel-Wagner, W. Maier, R. Hurlmann, Hormonal contraceptives suppress oxytocin-induced brain reward responses to the partner's face. *Soc. Cogn. Affect. Neurosci.* **11**, 767–774 (2016).
56. A. P. Borrow, R. J. Handa, Estrogen receptors modulation of anxiety-like behavior. *Vitam. Horm.* **103**, 27–52 (2017).
57. M. P. Paulus, The role of neuroimaging for the diagnosis and treatment of anxiety disorders. *Depress. Anxiety* **25**, 348–356 (2008).
58. J. LeDoux, The amygdala. *Curr. Biol.* **17**, R868–R874 (2007).

59. H. Geng, X. Li, J. Chen, X. Li, R. Gu, Decreased intra- and inter-saliency network functional connectivity is related to trait anxiety in adolescents. *Front. Behav. Neurosci.* **9**, 350 (2016).
60. D. V. Sheehan *et al.*, The Mini-International Neuropsychiatric Interview (MINI): The development and validation of a structured diagnostic psychiatric interview for DSM-IV and ICD-10. *J. Clin. Psychiatry* **59** (suppl. 20), 22–33, quiz 34–57 (1998).
61. E. MacDonald *et al.*, A review of safety, side-effects and subjective reactions to intranasal oxytocin in human research. *Psychoneuroendocrinology* **36**, 1114–1126 (2011).
62. R. Mandrioli, L. Mercolini, M. A. Raggi, Benzodiazepine metabolism: An analytical perspective. *Curr. Drug Metab.* **9**, 827–844 (2008).
63. D. Lundqvist, A. Flykt, A. Öhman, *The Karolinska Directed Emotional Faces-KDEF, CD-ROM*, (Department of Clinical Neuroscience, Psychology Section, Karolinska Institute, Stockholm, Sweden, 1998).
64. R. Stirnberg, D. Brenner, T. Stöcker, N. J. Shah, Rapid fat suppression for three-dimensional echo planar imaging with minimized specific absorption rate. *Magn. Reson. Med.* **76**, 1517–1523 (2016).
65. B. A. Poser, P. J. Koopmans, T. Witzel, L. L. Wald, M. Barth, Three-dimensional echo-planar imaging at 7 Tesla. *Neuroimage* **51**, 261–266 (2010).
66. K. J. Friston *et al.*, Statistical parametric maps in functional imaging: A general linear approach. *Hum. Brain Mapp.* **2**, 189–210 (1994).
67. K. Amunts *et al.*, Cytoarchitectonic mapping of the human amygdala, hippocampal region, and entorhinal cortex: Intersubject variability and probability maps. *Anat. Embryol.* **210**, 343–352 (2005).
68. S. B. Eickhoff *et al.*, A new SPM toolbox for combining probabilistic cytoarchitectonic maps and functional imaging data. *Neuroimage* **25**, 1325–1335 (2005).
69. D. G. McLaren, M. L. Ries, G. Xu, S. C. Johnson, A generalized form of context-dependent psychophysiological interactions (gPPI): A comparison to standard approaches. *Neuroimage* **61**, 1277–1286 (2012).